SCIENTIFIC Publishing Limited

New Energy Exploitation and Application

https://ojs.ukscip.com/journals/neea

Article

Optimizing Thermal Management: An Evaluation of Embedded Aluminum-Ammonia Heat Pipes Honeycomb Sandwich Panel as a Heat Sink for Satellite Use

Ho-Chuan Lin [1,*], Van-Hoan Vu [1], Alfandy Tansyafri [1] and Meng-Hao Chen [2]

[1] EW JET PRODUCTS Co., Ltd, New Taipei City 221451, Taiwan

[2] Taiwan Space Agency (TASA), Hsinchu Science Park, Hsinchu City 300091, Taiwan

[*] Correspondence: edlin@ewjpro.com

Received: 15 December 2023; **Revised**: 11 January 2024; **Accepted**: 12 January 2024; **Published**: 27 January 2024

Abstract: This study presents an innovative approach to enhancing thermal management in satellite applications by utilizing an embedded aluminum-ammonia heat pipes honeycomb sandwich panel (HPA-PNL) as a high-performance heat sink. The study focuses on developing and evaluating this advanced heat sink technology, addressing the challenges associated with assessing its performance and suitability for satellite use. The research explores the selection of materials and testing methodologies, highlighting the significance of overcoming existing limitations in the absence of standardized testing methods. The results of the thermal conductivity in Z-directions (K_Z) indicated that the areas on top of the heat pipes show higher thermal conductivity than those on top of the honeycomb core. Also, the effect of background heat sources and different kinds of thermal interface material (TIM) on HPA-PNL performance is insignificant. The heat dissipation through the heat pipe is substantial, emphasizing the effective ability to dissipate heat for an HPA-PNL with many heat sources acting simultaneously. The outcomes of this study reveal promising testing methods for evaluating the K_Z of the HPA-PNL, proposing the potential of the embedded aluminum-ammonia heat pipes honeycomb sandwich panel as a highly effective and efficient heat sink for satellite systems, thus contributing to the advancement of satellite technology.

Keywords: honeycomb core panel; aluminum ammonia heat pipe; heat sink; satellite radiator

1. Introduction

In today's fast-paced world satellites play a critical role in facilitating global communications. The development and enhancement of satellites become increasingly important as science and technology advances. Satellites now incorporate advanced technologies expanded operational ranges, reduced weight, and extended service life, reflecting the continuous effort to integrate leading-edge features. As a result, integrating numerous high-performance components within satellites underscores the pressing need for efficient thermal management solutions [1–3]. Addressing the critical demand for lightweight and highly effective heat rejection in the thermal management of satellite systems, the combination of honeycomb panels [4,5] and heat pipes (HP) [6–8] has been raised as a promising solution. Although the integral heat pipe honeycomb panel shows great potential, there are significant challenges not only in evaluating its performance and determining its application feasibility but also in establishing standardized testing methods to assess its effectiveness accurately. The absence of such standardized methods complicates the process of selecting an appropriate testing approach, further highlighting the intricate nature of advancing thermal management technologies in satellite systems. Efforts to overcome these challenges are crucial to ensure the successful integration and deployment of cutting-edge heat rejection solutions for the evolving needs of satellite technology [9,10].

Several testing methods for different types of panel and heat pipe designs from the past are reviewed. Ted et al. investigated materials and panel configurations, designing a lightweight heat pipe panel and subjecting it to a life test at 260 ℃ for 324 hours to assess its structural integrity [11]. Algerd B. et al. presented a test method

for the liquid metal heat pipe sandwich panel by radiant heat lamps [12]. Five pairs of thermocouples are placed on the top and bottom surfaces, and four more along one side of the panel to record the temperature gradient and startup performance.

Tanzer, H.J. extensively evaluated honeycomb core structures, as well as the core and face sheet materials, in the context of high-capacity honeycomb panel heat pipes designed for space radiators [13]. Besides, eleven honeycomb panel chamber prototypes using alkali metal fluids were fabricated, and an operational check on isothermality as an exploratory development was conducted [14]. A testing method for the embedded heat pipe composite sandwich panel is demonstrated by Chun-Liang L. et al. [15]. The panel's performance was measured using a film heater and two aluminum blocks as heat sinks in a vacuum chamber. Seven thermocouples are used to record the temperature of the heater, heat sinks, and the specimen.

However, the references above primarily focus on aspects such as panel design, material, and core structure, aiming to assess manufacturing feasibility, optimize panel mass, and enhance capacity. Yet, they lack guidance regarding the arrangement of heat generators when integrated into satellites. Besides, though these references were accessed and experimented with the relevance of a well-known agency, NASA, but they are outdated, while innovative testing methods with high levels of security are strictly regulated. This study seeks to address this gap by introducing a testing method to evaluate the panel's performance and generate a thermal conductivity map, establishing a standard for arranging satellite components. The research involves an examination of the use of aluminum ammonia heat pipe to create a heat sink for satellite applications, known as the embedded aluminum-ammonia heat pipes honeycomb sandwich panel (HPA-PNL).

2. Experimental Method

This chapter is divided into three sections that detail the tested specimen, testing systems, and equation for calculating results. First, the conceptual design section describes the geometric parameters and schematic of the HPA-PNL tested in this study. Second, the experiment configuration section then presents the testing equipment, setup, and testing scenarios. Lastly, the mathematical formulation section shows the formulae utilized to organize the obtained data.

2.1. Assembly Design

The design of the current HPA-PNL is illustrated in Figure 1, featuring dimensions of 700 × 350 × 18.6 mm. The HPA-PNL consists of 3 straight aluminum-ammonia axially grooved heat pipes (Al-AGHPs) are placed along the long side of the panel. Two types of honeycomb cores, consisting of two core A and two core B, are interspersed among the heat pipes, contributing to the structural composition. Two core A units are positioned on each side of the panel, while the two core B units are situated between the HPs. The face sheet is a 0.032-inch thick 7075 alloy material. Two layers of 3M AF-191K adhesive films serve as the interface between the face sheet and the layer comprising cores and heat pipes for both the top and bottom skins. The specific dimensions of all HPA-PNL parts are listed below in Table 1. The fabrication process involves directly embedding heat pipes into the panel utilizing the autoclave method.

2.2. Experiment Configuration

The experiment configuration, illustrated in Figure 2, describes the testing configuration for the thermal performance test of the HPA-PNL. The methodology involves the strategic placement of a rounded ceramic heater plate measuring Ø48 × 1.8 mm (represented by dotted circles) at five distinct positions denoted as A, B, C, D, and E. These positions are selected along the right-side heat pipe of the panel (A, D, and E), on top of the honeycomb core area (B), and the midsection of the panel's heat pipe (C). Each heat pipe was charged with an ammonia amount of 16 ± 0.2 g. Additionally, three supplementary heaters (shown as small rectangles) are incorporated to simulate the background temperature conditions of the HPA-PNL.

In this configuration, the panel's temperature aligns with the ambient temperature when the background heaters are turned off and assumes a predefined temperature when activated. With the performance of the three heat pipes being uniform, the purpose of this setup is to evaluate the thermal conductivity in the Z-direction (perpendicular to the HPA-PNL) and identify optimal locations to achieve a desired cooling rate for the electronic components housed on the satellite.

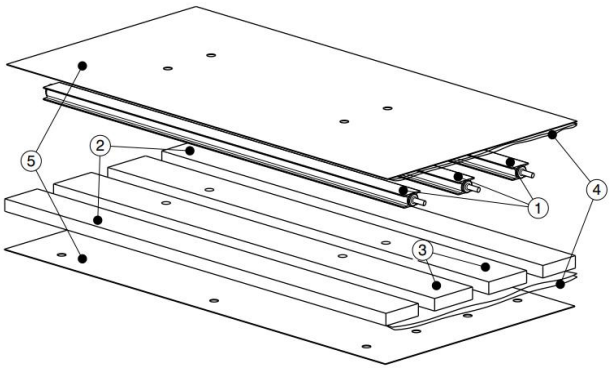

Figure 1. Schematic of the HPA-PNL.

Table 1. Part list of the HPA-PNL.

No.	Description	Dimension (mm)	QTY
1	Al-AGHP	650 × 30 × 17	3
2	Honeycomb core A	700 × 60 × 17	2
3	Honeycomb core B	700 × 70 × 17	2
4	Adhesive film	700 × 350	4
5	Face sheet	700 × 35 × 0.8128	2

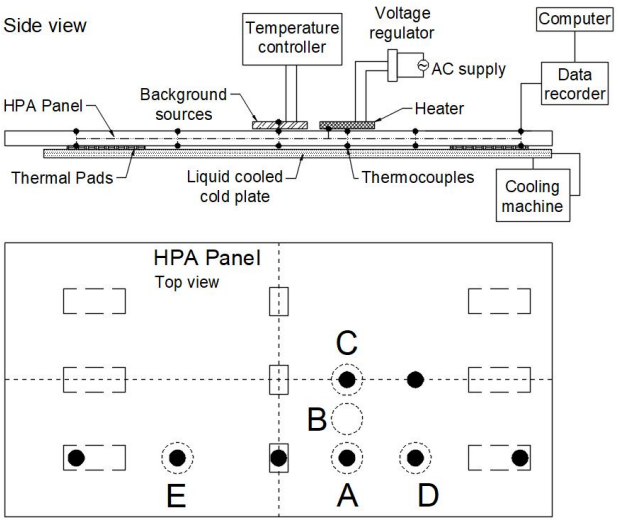

Figure 2. HPA-PNL experiment configuration.

The HPA-PNL was attached to a cooling plate with a dimension of 600 × 300 × 10 mm and secured with four bolts through the inserts. In between, six thermal pads (illustrated as dash rectangles) are utilized, each measuring 10 × 33 × 3 mm. The cooling plate is a liquid-cooled cold plate featuring a liquid loop channel, and the coolant liquid is a mixture of water and ethylene glycol (EG). The liquid channel was connected to a cooling machine to ensure a steady flow rate (30 L/min) and control the coolant liquid temperature. Sixteen designated points equipped with T-Type thermocouples were established for measurement: eight points positioned at the heater side (H1 to H8) indicated as the black dots in the Top view schematic and eight symmetric points at the cooling side (C1 to C8). A data recorder recorded the temperature that was detected by the thermocouples. Two additional thermocouples were employed to monitor the temperatures of the background sources and the heater. The background source temperature was set at 80 °C and regulated by a temperature controller. The input power was within the range of 20–100 W, while the cooling plate's temperature was kept at 0 °C.

The experiment configuration above is the test for a bad scenario with the heater placed at the top of the HPA-PNL—defined as setup 1. Another configuration for the good scenario is the upside-down of the bad scenario. Also, in the good scenario test, two kinds of thermal interface materials (TIM) are used to compare if there is any difference in the HPA-PNL's performance. They are defined as setup 2, with the use of the thermal pads and setup 3, with the use of the thermal grease. Thermal grease is applied in the same area as the thermal pads with a thickness of 1mm. The thermal conductivity of the thermal pad is 7.2 W/mK, and the thermal grease is 7.5 W/mK.

2.3. Mathematical Formulation

The average temperature of each thermocouple position (x) at the evaporator side ($\overline{T_{ex}}$) with the placement of the heater and condenser side ($\overline{T_{cx}}$) with the placement of the cold plate, shows the temperature distribution of the HPA-PNL when the HP has reached a steady state. The first 50 seconds of data after each time the Q_{in} adjusted are excluded from the average calculation, as stated in the Equation (1) below.

$$\overline{T_{ex}} = \sum_{i=51}^{n} \frac{T_{exi}}{n-50} \qquad \overline{T_{cx}} = \sum_{i=51}^{n} \frac{T_{cxi}}{n-50} \tag{1}$$

The temperature difference between the evaporator and condenser sides at each thermocouple position indicates the thermal performance of the HPA-PNL when the HP reaches a steady state. The average delta T is shown in the Equation (2) below:

$$\overline{\Delta T_x} = \overline{T_{ex}} - \overline{T_{cx}} \tag{2}$$

With power input of the heater (Q_{in}), the thickness of the HPA-PNL (L), and heating area (A). The equation for the thermal conductivity in Z-directions (K_Z) can be expressed as Equation (3):

$$K_Z = \frac{Q_{in} \times L}{A \times \overline{\Delta T_x}} \tag{3}$$

3. Results

Heat pipes were tested horizontally before being embedded into the HPA-PNL. During the test, the evaporator and condenser were placed at two ends of the HP with an effective length (L) of 173 mm. The obtained longitudinal K_{eff} of each HP falls within the range of 130 ± 10 kW/mK at Q_{in} = 300 W.

For the HPA-PNL, testing was exclusively conducted on the right and center heat pipes, while background source tests were specifically executed with the heater positioned at point A. The K_Z of the panel at various heater positions is described in Figure 3. It is shown that the K_Z increases equivalently with the rise in input power. The highest K_Z is recorded at point C—the middle HP, followed by points D, E, and A, respectively. The range for K_Z at point C spans from 20.01 W/mK at 20 W to 22 W/mK at 100 W. Conversely, at point B—on the honeycomb core, the thermal conductivity is lowest, measuring 11.9 W/mK at 20 W and 13.95 W/mK at 100 W.

Furthermore, activating the background sources has negligible impact on the HPA-PNL performance when compared to their inactive state, with K_Z between 17.85–19.7 W/mK from 20 to 100 W when background sources are off (Point A) and 17.4–19.35 W/mK when they are on (Point A + BG).

The comparison of K_Z between the good and bad scenarios with the heater positioned at point A is illustrated in Figure 4. Particularly, the HPA-PNL's performance is significantly higher in the good scenario (20.1 –27.6 W/mK) compared to the bad scenario (17.85–19.68 W/mK). Additionally, the performance difference between the thermal pad with K_Z ranging from 21.3 to 26.8 W/mK and thermal grease with K_Z ranging from 20.1 to 27.6 W/mK is small. It can be explained by the negligible difference in the thermal conductivity between the two TIMs.

Utilizing the obtained results for average thermal conductivity and temperature distribution, Figure 5 displays a K_Z map in different scenarios. The optimal positions for placing chips or other heat sources with elevated working temperatures are identified in the midsection of the panel and a contiguous small area. To sustain a balanced temperature distribution across the panel, it is advisable to position chips or other heat sources with lower working temperatures on the heat pipes at the panel's two sides. The red zone on the map signifies suitable locations for heat sources with the TIMs applied in these areas, while the green zones indicate areas that should be avoided due to the low thermal conductivity of the honeycomb structure. This mapping provides valuable insights for optimizing the placement of heat-generating components on the panel to enhance overall thermal performance.

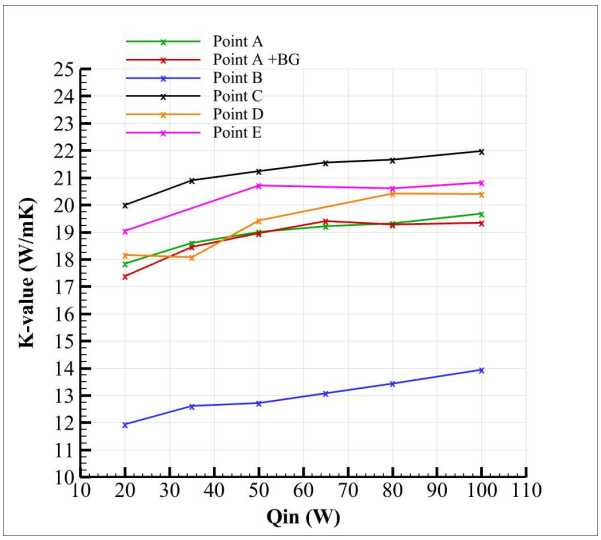

Figure 3. K_Z comparison of the HPA-PNL with the heater at different positions in a bad scenario.

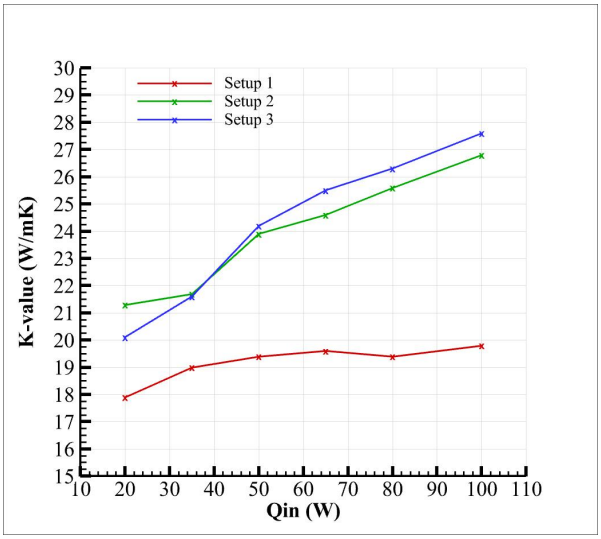

Figure 4. Average K_Z comparison with different test setups. Setup 1) Heater on top of the HPA-PNL; Setup 2) Heater at the bottom of the HPA-PNL, the used TIM is thermal pads; Setup 3) Heater at the bottom of the HPA-PNL, the used TIM is thermal grease.

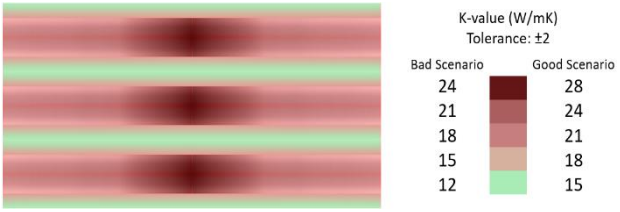

Figure 5. K_Z map of the HPA-PNL for the heat source placement.

4. Discussion

The findings from the conducted experiments, involving the assessment of thermal conductivity and temperature distribution, concluded in the creation of a K_Z map. The map serves as a valuable tool for guiding the placement of heat-generating components, such as chips or other heat sources, on the HPA-PNL. Moreover, the

heat mainly concentrates on an HP where the heat source is placed. Therefore, a reasonable arrangement of the heat source helps not only the lifetime of the working devices on the satellite but also the HPA-PNL itself.

The panel's thermal conductivity in the Z direction is equivalent to the input power, demonstrating an increase with higher power levels. The values of K_Z at different heater positions reveal that the midsection of the panel, specifically point C, exhibits the highest thermal conductivity, followed by points D, E, and A, respectively. This could also imply that the middle section of the HPA-PNL is more effective. Conversely, the honeycomb core at point B exhibits the lowest thermal conductivity, making it less conducive to heat dissipation.

Moreover, the HPA-PNL's performance is taken into account with background sources activated. The results from Figure 3, the K_Z show negligible differences, proving that the heat load could be extracted by the HP relatively quickly. Additionally, comparing the good and bad scenarios gives a better view of how the working conditions could affect the HPA-PNL's performance. The negligible difference in the performance between thermal pads and thermal grease also highlighted the importance of material selection in achieving optimal thermal rejection.

Utilizing the obtained results, a K_Z map is presented in different scenarios, offering insights into optimal positions for placing heat-generating components. The areas on top of the heat pipe positions and the contiguous small areas are identified as optimal positions for chips with elevated working temperatures, while other heat sources with lower working temperatures are recommended for the panel's two sides. The map illustrates suitable locations (red zones) and areas to avoid (green zones) based on the thermal conductivity of the honeycomb structure. This mapping provides valuable guidance for optimizing the placement of heat-generating components to enhance the overall thermal performance of the HPA-PNL.

5. Conclusions

In conclusion, this research contributes a detailed testing method for an Embedded Aluminum-Ammonia Heat Pipes Honeycomb Sandwich Panel (HPA-PNL) to overcome the limitation in the absence of standardized testing methods by judging the thermal conductivity of the panel in various positions and working conditions. The experiments focused on assessing the Z-direction thermal conductivity and temperature distribution of the HPA-PNL, providing valuable insights for optimizing the thermal management of satellite systems. The results indicate a relatively fast heat dissipation along the heat pipe of the HPA-PNL, demonstrating its high heat exchange capacity. Additionally, the Z-direction conductivity results are similar to those of industrial TIM, indicating that the bonding structure of the HPA-PNL is good.

Moreover, the results underscore the significance of the K_Z map in guiding the strategic placement of heat-generating components for optimal thermal management in satellite applications. The concentration of heat on the heat pipe corresponding to the placement of the heat source emphasizes the critical role of proper arrangement in not only extending the lifetime of working devices on the satellite but also enhancing the overall durability of the HPA-PNL itself.

The negligible impact of background source activation on the HPA-PNL's performance, as evidenced by minimal differences in K_Z values, indicates the potential of the panel to handle a lot of acting heat sources simultaneously. Besides, comparing good and bad scenarios provided a comprehensive view of how working conditions could impact the HPA-PNL's performance. The minimal difference in performance between thermal pads and thermal grease emphasized the critical role of material selection in achieving optimal thermal rejection, underlining the importance of considering material properties in designing and implementing advanced thermal management solutions for satellite systems. Overall, these findings contribute significantly to the ongoing efforts to enhance the efficiency and reliability of satellite technologies.

In essence, these findings contribute significantly to advancing the understanding of thermal management in satellite systems, offering practical recommendations for optimizing heat dissipation strategies and ensuring the longevity and reliability of satellite technologies in varying operational scenarios. Further research and development in this direction hold the potential to refine and innovate thermal solutions for the evolving needs of satellite technology.

Author Contributions

The authors confirm their contribution to the paper as follows: Supervision: Ho-Chuan Lin, Meng-Hao Chen; data collection: Van-Hoan Vu; analysis and interpretation of results: Alfandy Tansyafri, Van-Hoan Vu. All authors reviewed the results and approved the final version of the manuscript.

Conflicts of Interest

The authors declare no conflict of interest.

Nomenclature

A	Area	[m^2]
K	Thermal conductivity	[W/mK]
K_{eff}	effective thermal conductivity of HP	[W/mK]
L	Length	[m]
Q_{in}	Heat power	[W]
Q_{max}	Maximum heat power	[W]
R	Thermal resistance	[K/W]
T	Temperature	[°C]
a	adiabatic	
c	condenser	
cool	cooler machine	
e	evaporator	
in	input	

References

1. Pisacane, V.L. *The Space Environment and Its Effects on Space Systems*, 2nd ed.; American Institute of Aeronautics and Astronautics: Reston, US, 2016; pp. 771–852.
2. Ponnappan, R.; Donovan, B.; Chow, L. High-power thermal management issues in space-base systems. *AIP Conf. Proc.* **2002**, *608*(1), 65–72. [CrossRef]
3. Mccabe, M.E.; Ku, J.; Benner, S. *Design and Testing of a High Power Spacecraft Thermal Management System*; National Aeronautics and Space Administration: Washington D.C., US, 1988.
4. Darji, J.J. Heat Transfer Through a Honeycomb Sandwich Panel. Master's thesis, School of Mines and Metallurgy of the University of Missouri, Rolla, Missouri, 1963.
5. Nguyen, D.D. Analysis and Testing of Heat Transfer through Honeycomb Panels. Master thesis, California Polytechnic State University, San Luis Obispo, CA, US, May 2012.
6. Zohuri, B. *Heat Pipe Design and Technology: Modern Applications for Practical Thermal Management*, 2nd ed.; Springer International Publishing: AG, Switzerland, 2016.
7. Kappe, K.; Bihler, M.; Morawietz, K.; Hügenell, P.P.C.; Pfaff, A.; Hoschke, K. Design Concepts and Performance Characterization of Heat Pipe Wick Structures by LPBF Additive Manufacturing. *Materials* **2022**, *15*(24), 8930. [CrossRef]
8. Tang, H.; Tang, Y.; Li, J.; Sun, Y.; Liang, G.; Peng, R. Experimental Investigation of the Thermal Performance of Heat Pipe with Multi-Heat Source and Double-End Cooling, *Appl. Therm. Eng.* **2018**, *131*, 159–166. [CrossRef]
9. Fortescue, P.; Swinerd, G.; Stark, J. *Spacecraft Systems Engineering*, 4th ed.; John Wiley & Sons, Inc.: New York, US, 2011.
10. Bejan, A.; Kraus, A.D. *Heat Transfer Handbook*; John Wiley & Sons, Inc.: New York, US, 2003.
11. Stern, T.; Anderson, W.G. High Temperature Lightweight Heat Pipe Panel Technology Development. In Proceeding of the Space Nuclear Conference, San Diego, California, 5–9 June 2005.
12. Basiulis, A.; Camarda, C. Design, Fabrication and Test of Liquid Metal Heat-Pipe Sandwich Panels. In Proceeding of the AIAA/ASME 3rd Joint Thermophysics, Fluids, Plasma and Heat Transfer Conference, St. Louis, Missouri, 7–11 June 1982.
13. Tanzer, H.J. High Capacity Honeycomb Panel Heat Pipes for Space Radiators. In Proceeding of the AIAA 18th Themophysics Conference, Montreal, Canada, 1–3 June 1983.
14. Fabrication and Development of Several Heat Pipe Honeycomb Sandwich Panel Concepts. Available online: https://ntrs.nasa.gov/api/citations/19830002109/downloads/19830002109.pdf.
15. Lin, C.L.; Choi, J.H.; Dharant, C.K.H. Thermal Performance of Embedded Heat Pipe Composite Sandwich Panels. In Proceeding of the AIAA 40th Structures, Structural Dynamics, and Materials Conference and Exhibit, St. Louis, Missouri, 12–15 April 1999.